N90-26477

EXPERIMENT K-6-24, K-6-25, K-6-26

RADIATION DOSIMETRY AND SPECTROMETRY

Principal Investigator:

E.V. Benton
Physics Research Laboratory
University of San Francisco
San Francisco, California

Co-Investigators:

A. Frank,
E.R. Benton
University of San Francisco
San Francisco, California

V. Dudkin
A. Marennyi
Institute of Biomedical Problems
Moscow, USSR

PRECEDING PAGE BLANK NOT FILMED

SUMMARY

Radiation experiments flown by the University of San Francisco on the Cosmos 1887 spacecraft were designed to measure the depth dependence of both total dose and heavy particle flux, dose and dose equivalent, down to very thin shielding. Three experiments were flown and were located both inside and outside the Cosmos 1887 spacecraft. Tissue absorbed dose rates of 264 to 0.028 rad d^{-1} under shielding of 0.013 to 3.4 g/cm^2 of ^{7}LiF were found outside the spacecraft and 0.025 rad d^{-1} inside. Heavy particle fluxes of 3.43 to 1.03 x 10^{-3} cm $^{-2}s^{-1}sr^{-1}$ under shielding of 0.195 to 1.33 g/cm^2 plastic were found outside the spacecraft and 4.25 x 10^{-4} cm $^{-2}s^{-1}sr^{-1}$ inside ($LET_{\infty}H_2O \geq 4$ keV/μm). The corresponding heavy particle dose equivalent rates outside the spacecraft were 30.8 to 19.8 mrem d^{-1} and 11.4 mrem d^{-1} inside. The large dose and particle fluxes found at small shielding thicknesses emphasize the importance of these and future measurements at low shielding, for predicting radiation effects on space materials and experiments where shielding is minimal and on astronauts during EVA.

The Cosmos 1887 mission contained a variety of international radiobiological investigations to which the measurements apply. The high inclination orbit (62°) of this mission provided a radiation environment which is seldom available to U.S. investigators. The radiation measurements will be compared with those of other research groups and also with those perf .med on the Shuttle, and will be used to refine computer models employed to calculate radiation exposures on other spacecraft, including the Space Station.

INTRODUCTION

The Soviet Cosmos 1887 biosatellite mission was host to a wide variety of space biology and radiation experiments performed by several research groups. Included were three sets of radiation dosimetry and spectrometry experiments flown by the University of San Francisco (USF). Experiments employed passive detectors for heavy cosmic ray, proton, neutron and total dose measurements. The radiation environment both inside and outside the spacecraft was monitored, with particular emphasis on shielding depth dependence and including very small shielding thicknesses.

The Cosmos 1887 experiments follow from previous USF participations in the Cosmos series (on mission Nos. 782, 936 and 1129 /Peterson, et al., 1978; Benton, et al., 1978a; Benton, et al., 1978b; Benton, et al., 1981; Kovalev, et al., 1981/) as well as a wide range of U .S. space flights, including the Gemini, Apollo, Skylab, Apollo-Soyuz and Space Shuttle missions /Benton, et al., 1977a; Benton, et al., 1977b; Benton and Henke, 1983; Benton, 1984; Benton, et al., 1985; Benton, 1986; Benton and Parnell, 1987. In addition to providing radiation measurements specific to the mission and its experiments, the acquired data adds to the long-term project of mapping radiation intensities in near-Earth orbit and in providing measured comparisons for the radiation modeling codes. The Cosmos 1887 mission also offered the opportunity to intercompare measurements with other research groups and in this way compare measurements of some quantities (i.e. dose, LET) using different techniques.

EXPERIMENTS

The three Cosmos 1887 experiments are discussed individually below.

Experiment K-6-24

The objective of this experiment was to measure the radiation environment inside the spacecraft. We were able to obtain only a very approximate idea of the shielding, but useful comparisons of dose rates and LET spectra can be made with experiments positioned on the outside of the spacecraft as well as with measurements made on previous spaceflights. The detectors used were plastic nuclear track detectors (PNTDs), nuclear emulsions and thermoluminescent detectors (TLDs).

Five PNTD stacks were used to measure the heavy-particle, high LET spectra, a nuclear emulsion stack was included to measure the energetic proton spectrum, and TLDs (TLD-700) were used to measure the total dose. The components were placed in a Lexan polycarbonate plastic box (7 cm x 7 cm x 3.95 cm), with the five PNTD stacks (one thick center stack plus four thin side stacks) arranged in an orthogonal array to compensate for the angular response of PNTDs. The PNTDs used were special, high-sensitivity CR-39, developed in

this laboratory, plus several sheets of Tuffak polycarbonate detector. The physical dimensions of the detectors and their configuration in the Lexan box are shown in Figures 1 - 4.

Experiment K-6-25

The objective here was to measure the depth dose under very thin shielding on the outside of the spacecraft and to determine what fraction of the dose was due to low energy electrons versus heavy charged particles. This required that the shielding of the outermost detectors be no more than a few mg/cm^2 and that the detectors themselves also be very thin (because of the short ranges of the particles). The maximum depth in the TLD stacks was 3.4 g/cm^2. Although computer codes exist for calculating doses encountered in LEO both from protons and electrons, there have been only a few instances where a direct comparison (under very thin shielding) has been possible between experiment and theoretical prediction.

Two identical flight units (F1 and F2) each containing three stacks of TLDs were used. F1 and F2 consisted of aluminum cylinders of 5 cm diameter and 1.99 cm thickness with cylindrical holes to accommodate TLD stacks. In two stacks (Nos. 1 and 2), thin (9.14 x 10^{-3} cm) TLDs were placed at the tops, and thicker (0.889 mm) TLDs at the bottoms. In the third stack only the thicker (0.889 mm) TLDs were used. An aluminized double-window of Kapton plastic totaling 15 μm served to hold in the TLD stacks and to protect them from direct sunlight, heat and vibration. Each aluminized surface had an optical density of 3. In addition to the three USF stacks, a center hole was placed in the cylinders and left open for use by the Soviets. The detector unit configuration is shown in Figure 5.

In the stacks with only the thicker TLDs (No. 3) there were sixteen ^{7}LiF TLDs, with separators of 15 μm-thick polycarbonate film between the detectors for protection against vibration and movement. Strips of stiff 0.015 cm-thick paper were inserted along all four sides and the bottoms of the stacks to hold the TLDs in vertical alignment and give further protection against mechanical effects.

In the stacks with thin TLDs (Nos. 2 and 3) there were 30 thin chips at the top, and 12 thicker chips underneath. All TLDs were ^{7}LiF and were separated by 15 μm-thick polycarbonate film, as above. Paper was placed beneath each stack but could not be inserted along the sides of the stacks because of the fragility of the thin TLDs. The K-6-25 units were mounted on the outside of the spacecraft, with the No. 2 flight cylinder being partially shielded by the spacecraft auxiliary battery power unit which is also externally mounted.

Experiment K-6-26

Part A:

The objective here was to measure the low energy, heavy particle (excluding electrons) LET spectra under essentially zero shielding (outside the spacecraft) and as a function of depth. Although there have been some previous measurements of LET spectra under such conditions, the orbital dependence and the effects of solar cycle on the low energy charged particle component are still not well understood.

The hardware consisted of two hermetically sealed flight units containing PNTD stacks and with aluminized Kapton double-windows, as in Experiment K-6-25. The PNTD stacks were 3 cm in diameter and 1.4 cm thick and included sets of CR-39, Tuffak polycarbonate and Cronar polyester detectors. The physical configurations of the units and PNTD stacks are shown in Figures 6 and 7.

Parts B and C:

Here the intent was to obtain some information on the neutron energy spectra. Part B detectors were located on the outside of the spacecraft and Part C on the inside.

Part B of the experiment consisted of two flight units containing ^{59}Co activation foils and PNTD films. An aluminum frame with aluminized Kapton double-windows was placed above the detectors but the sides of the units were open to vacuum. The PNTDs used were Tuffak polycarbonate and Cronar polyester. The purpose of the PNTDs in this experiment was for an intercomparison between those open to vacuum and those

hermetically sealed. Due to space limitations, CR-39 was not included. The configuration of the units is shown in Figure 8.

Part C consisted of a single ^{59}Co activation foil. This foil was placed inside the spacecraft near Experiment K-6-24.

The selection of available isotopes with suitable activation cross sections and decay product half-lives for spaceflights of a few days places severe limitations on this method. Cross sections exist for the measurement of both low energy (thermal plus resonance) and high energy (>10 MeV) neutrons, with some proton contribution, with the activations forming ^{60}Co and ^{58}Co. However, readout requires a very sensitive, low background spectrometer.

Detector Exposure:

Cosmos 1887 was launched on September 29, 1987, re-entry was on October 12, 1987, for a flight duration of 12.634 days. Orbit inclination was 62.8°, while apogee/perigee were 406 km/224 km.

The K-6-25 and K-6-26 A and B units were mounted on the outside of the spacecraft, inside flat, lidded containers (see Figure 9). The container lids were open during takeoff and while in orbit, but were closed before re-entry.

The flight and ground-control units were returned to our laboratory on October 24, 1987, in generally good condition, although the K-6-26 B units were blemished. Unit B-F1 had a residue of some material beaded on the surface which had apparently become hot. When disassembled, the PNTDs inside unit B-F1 appeared warped, as though they had become hot. Unit B-F2 had the upper of the two aluminized windows mostly torn off. The ^{59}Co activation foils were unaffected by the above.

The paper strip temperature indicators in the K-6-26 A units gave maximum temperature readings between 40.6°C and 46°C (unit A-F1) and between 77°C and 88°C (Unit A-F2). The duration of the high temperature excursions is not known.

Processing and Readout:

Plastic Nuclear Track Detectors (PNTDs):

The CR-39, the polycarbonate and the polyester PNTDs were given standard processing in 6.25N NaOH solution at 50°C. The bulk etch, B, (single surface thickness) of each of the films was measured. Preliminary scanning showed that the track densities on the polycarbonate and polyester detectors were very low (<1 cm^{-2}) while the CR-39 track densities were much higher (~400-2000 cm^{-2}). Pairs of CR-39 films were reassembled in their flight configurations. The scanning took place on the two interior surfaces of the pairs. This enabled the particles to be separated into short range (SR): matching tracks appearing on only the two interior surfaces, and long range, galactic cosmic rays (GCR): matching tracks appearing on all four surfaces of the pair of films. The major and minor axes of the eliptical surface openings of tracks were measured. The axial measurements, together with the "B" of the samples and the calibrated LET response function of the CR-39 material, were then used to generate particle LET spectra.

Thermoluminescent Dosimeters (TLDS):

The TLDs were read out using a Harshaw Model 4000 TLD Reader. A 30-sec read cycle and 10°C/sec temperature ramp were employed. The total glow peak distributions were recorded by data transfer to a microcomputer, which makes possible glow peak deconvolution. This was accomplished with the Harshaw Data File Management System microcomputer software.

TLDS from the flight and ground control units and ^{137}Cs source standard irradiations were read out together. This allowed the proper background subtractions and conversion of TLD signal to absorbed dose.

^{59}Co Activation Foils:

For relatively short spaceflights of a few days there are four reactions to consider in the use of ^{59}Co activation foils. These are ^{59}Co(n,g) ^{60}Co, ^{59}Co (n,2n)^{58} Co, ^{59}Co(p,np) ^{58}Co, and ^{59}Co(n,p) ^{59}Fe. The (n,g) reaction has cross sections of 37.4 barns for thermal neutrons and a resonance integral of 77 barns for 132 eV. The 5.27 y half-life of ^{60} Co is, however, much longer than optimum. The (n,2n) reaction cross section has a maximum of about 800 mb between 17 and 20 MeV, but the 71.3 d half-life of ^{58} Co is much closer to optimum. The (p,np) reaction also yields ^{58} Co so there is a possibility of a mixed contribution from protons and neutrons. The proton ranges in a thick ^{59}Co foil will also complicate this analysis. The (n,p) reaction cross section is about 750 mb in the 14 MeV region. The ^{59}Fe half-life is 45 d, which is favorable.

It was planned that the ^{59}Co foils would be read out using a high sensitivity, very low background gamma ray spectrometer at the Manned Spaceflight Center near Huntsville. Unfortunately, the crystal of the spectrometer broke during the initial part of this procedure. The foils were transferred to a second facility having a spectrometer but this instrument had less favorable ratios of sensitivity to background. The counting results were negative in that the differences between the sample counts and the background were not statistically significant.

Nuclear Photographic Emulsions:

Nuclear emulsions have been processed and are still undergoing analysis.

RESULTS

Experiment K-6-24

The TLDs yielded a flight dose of 313 ± 13 mrads. This is compared below with the doses measured outside the spacecraft.

The CR-39 PNTDs yielded the integral particle LET flux spectra plotted in Figure 10, where the total (TOT) is the sum of GCR and SR spectra. The long-range (four-surface) tracks are due to GCRs and their projectile fragments, with the protons not included. The registration range of protons in this type of CR-39 is not sufficiently high to produce tracks on all four surfaces when the thickness of foils equals ~650 μm. The short range tracks therefore include all primary and secondary stopping protons and all higher Z stopping particles with a range ≤1300 μm in CR-39. The latter are mainly secondary particles produced from target nuclei within the PNTDs which have undergone interactions with energetic primaries (mainly protons).

Experiment K-6-25

Absorbed dose measurements in the TLD stacks from the F1 and F2 units are plotted in Figures 11, 12, and 13. The doses from the two stacks containing thin TLDs in each flight unit are plotted together in Figures 11 and 12. In the range of 0 to 1 g/cm^2 shielding thickness, the slope in the depth dose rate distribution is very steep and does rate may decline by ~4 orders of magnitude. The rate of change is greatest at the outer surface, where the very short range particles are absorbed. The doses from the thick TLD stacks in both of the flight units are plotted in Figure 13.

In Figures 11 and 12, curves have been fitted to the maximum doses at the tops of the stacks, to the doses from the thicker TLDs at the bottoms of the stacks, and to the lowest of the intermediate TLD doses. Most of the thinner TLD doses scatter above the curves. This is because the thinner TLD chips were not in precise vertical alignment. The small mass of these chips, together with springiness and electrostatic effects in the polycarbonate plastic separator films, caused horizontal displacements of the chips as they were stacked. The fragility of the thinner chips did not permit forcing them into alignment with inserts along the sides.

The magnitudes of the positive deviations in the measured absorbed doses are explained by the strong attenuation of the radiation entering through the tops of the stacks, while the radiation passing through the circular openings, but to the sides of the stacks, is less attenuated. Thus a small portion of a TLD chip extending out could contribute more to the total TLD signal than the much larger portion of the chip which lay within the stack boundary.

The thicker TLD chips (0.889 mm) at the bottoms of these stacks, and those within the stacks composed only of the thicker chips, were in a good alignment and do not show much scattering of data. The lower doses through which the curves were drawn represent those TLDs which were well-shielded from above. The curves give the best representations of the true depth-dose profiles. The depth-dose profiles measured only with the thicker TLDs show that the dose averaging of thick TLDS at low shielding thicknesses produces inaccurate results. There is also dose averaging for the thinner TLDs and, if thinner than 90 μm detectors were available, the maximum measured dose would have been higher.

Measured dose rates as a function of depth are also shown in Table 1, along with the K-6-24 data. In measuring dose versus depth in the TLD stacks, the polycarbonate plastic separator films were converted to equivalent ^{7}LiF thickness on the basis of the ranges of 10 MeV protons in the two materials (1 μm polycarbonate = 0.54 μm ^{7}LiF). It was observed that the dose rates at the bottoms of the TLD stacks (3.4 g/cm^2) located outside the spacecraft approached those found in the interior of the spacecraft.

The doses measured by the thicker TLDs (the No. 3 stacks) are seen to be higher than for the smaller type (No. 1 and 2 stacks), even above 1 g/cm^2 depth where dose averaging is not a problem. This occurs because of the larger horizontal dimensions of the TLDs in the No. 3 stacks (0.635 cm x 0.635 cm versus 0.318 cm x 0.318 cm). Larger diameter holes in the aluminum were necessary to accommodate the No. 3 stacks, which decreased the total 4π shielding around the stacks. The large holes are also slightly closer to the sides of the aluminum cylinders and to the center hole.

Experiment K-6-26

Part A:

To date, only the CR-39 detectors have undergone analysis. In the assembly of the two PNTD flight stacks, CR-39 pairs were alternated with the other films. Most of the thickness of the stacks consisted of CR-39. In the flight No. 1 stack the first CR-39 sheet had 0.0444 g/cm^2 of plastic above it. In the flight No. 2 stack the first CR-39 sheet had only the Kapton plastic double-window above it (0.00216 g/cm^2). When samples were processed, the upper surface of this least-shielded CR-39 film pitted very badly, showing that it must have been damaged by heat or by the high dose of low energy electrons. This layer could not be analyzed so the least-shielded detector layer was lost.

Integral LET flux spectra measured at four progressive depths in the F1 PNTD stack are plotted in Figures 14, 15, 16 and 17. The mass thicknesses of plastic shielding varied from 0.195 to 1.33 g/cm^2. The spectra are plotted for Total, GCR and SR as discussed previously. The SR and Total particle fluxes are variable. The GCR fluxes decrease, then increase again with increasing shielding depth. The decrease in the SR flux with depth is apparently due to a progressive stopping of primary short range particles, mainly protons, with depth. Most of the difference in the SR LET spectra is in the low LET region (<20 keV/μm), which supports the theory that low energy protons are the cause. If substantial numbers of primary particles with $Z \geq 2$ were stopping they would add to the GCR (four-surface tracks) spectra at the smaller depths. The increase in the GCR flux with depth is less easy to explain. This may be due to a slowing down of energetic primary particles, with a net increase in registered particles from the lighter nuclei which were initially outside the sensitive LET range of the CR-39. Another possibility is that energetic secondary alpha particles are produced with ranges greater than 1300 μm in CR-39. This would require energies ≥ 50 MeV. Secondaries of this type would increase the numbers of four-surface tracks with increasing depth until equilibrium between production and stopping was reached.

The LET spectra measured outside the spacecraft can be compared with that measured inside (K-6-24, Figure 10). The LET integral flux for the more heavily shielded inside detector is less than the outside fluxes for both the GCR and SR spectra. However, the GCR spectrum is lower over the full LET range

while the SR spectrum is lower only in the lower LET region. The SR spectrum inside the spacecraft is approximately equal to or greater than the outside spectra at LETs above 20 keV/μm. The effect of shielding on the PNTDs inside the spacecraft is therefore a continuation of the effect seen in the external stack where the SR spectrum is concerned.

The primary proton region in the SR spectra appears to lie below LETs of 20 keV/μm when, in fact, the maximum LETs for protons are 94.3 keV/μm (at 0.1 MeV). There are fundamental reasons for this. The LET region of 5-20 keV/μm corresponds to proton energies of 9-1.5 MeV and ranges in CR-39 plastic of 806-37 μm. LETs above 20 keV/μm correspond to proton ranges the section of a stopping proton track with LET >50 keV/μm is only about 4.5 μm in length R-39 detectors were processed, about 39 μm thickness of material was etched from each su ETs which are measured are the range-weighted average LET values within the etched laye track detection condition which was imposed in scanning the samples, that the particle be detec o adjacent surfaces, means that the particles needed a minimum range of about 85 μm in order to be counted. Since primary particles entering the tops of the PNTD stacks passed progressively through the Nos. 1, 2, 3, and 4 surfaces of each CR-39 pair, since the track parameters for the LET determinations were measured in the No. 2 surfaces, and since the corresponding tracks in the No. 3 surfaces were required for confirmation, then the sections of these tracks which determined the LETs were distant from the stopping points by a distance ≥ 45μm (this includes the 7 μm equivalent thickness of a polycarbonate separator foil between the two CR-39 films). This would yield a maximum LET of 17.4 keV/μm for measurements of these proton tracks. Given the LET resolution of CR-39 in this region, for isotropic particles (~10%), this is in reasonable agreement with the measurements. It should be noted that protons traveling in the opposite direction (up from the bottoms of the PNTD stacks) could yield higher measured LETs (up to ~35 keV/μm).

With regard to the 87 μm particle range cutoff mentioned above (the effective range cutoff for isotropic particles is greater), it should also be noted that the shorter range particles which intersect the detector surfaces are lost to the analysis and to the LET spectra. This will include a small fraction of the stopping primary particles (~6%) and perhaps a substantial fraction of secondary particles.

The integral fluxes, dose rates and dose equivalent rates for Total, GCR and SR particles and for six CR-39 detectors are given in Table 2. The steep decline in SR flux with depth in shielding is shown but it can also be seen that the dose rate and dose equivalent rate do not decrease as rapidly as flux, showing that the major difference is at the lower LETs. It is also interesting to note that the GCR flux is relatively high for the least shielded detector, drops substantially for the next least shielded, then builds up through the remainder of external stack No. 1. This suggests that the primary particles included a component with sufficient range and charge ($Z \geq 2$) to form four-surface tracks, but which was substantially absorbed in <0.4 g/cm^2 of plastic. Because the GCR fluxes were less than the SR, the statistical reliability of the GCR data is also less and this conclusion is tentative. However, in comparing the spectra, the least shielded GCR spectrum is somewhat higher than the others in the region of 100-200 keV/μm.

DISCUSSION

Results for Cosmos 1887 and a summary of data for three previous Cosmos flights are shown in Table 3. The differences in the heavy particle fluxes due to the more sensitive PNTDs used on Cosmos 1887 are quite large. The TLD doses inside the spacecraft are comparable for the different flights.

Total tissue absorbed dose rates on Cosmos 1887 varied from 264 to 0.028 rad d^{-1} under shielding of 0.013 to 3.4 g/cm^2 of ^{7}LiF outside the spacecraft and 0.025 ± 0.001 rad d^{-1} inside the spacecraft. The measurements of high LET particles ($LET_{\infty}H_2O \geq 4$ keV/μm^{-1}) show particle fluxes up to 3.43 x 10^{-3}cm^{-2}s^{-1}sr^{-1} outside the spacecraft and 4.25 x 10^{-4}cm^{-2}s^{-1}sr^{-1} inside. High LET dose rates and dose equivalent rates up to 5.25 mrad d^{-1} and 30.8 mrem d^{-1} were obtained outside the spacecraft, and rates of 1.27 mrad d^{-1} and 11.4 mrem d^{-1} were found inside. Because of damage to the least shielded CR-39 PNTD, the maximum levels of high LET particles were not obtained.

The LET spectrum from the K-6-26 A Flight No. 1 PNTD stack, layers 11 and 12, is shown as "crosses" in Figure 18 and compared with data from previous flights (Benton and Parnell, 1988). The minimum shielding of the detector was 0.436 g/cm^2 of plastic. The spectrum compares well with Soviet results from

Cosmos 782 and 936 and, in the higher LET region, Cosmos 1129. (These three flights all had similar orbits). The shielding of the electronic LET spectrometer used only by the Soviets on Cosmos 782, and presumably for the same type on 936, was only about 1 g/cm^2, while the shielding of their nuclear emulsions used on Cosmos 1129 was about 20 g/cm^2. This would account for the smaller fluxes seen on Cosmos 1129 for LET <20 keV/μm, which is in agreement with the effect of shielding reported in this paper.

An aspect of the K-6-25 experiment which needs to be improved for future measurements is in the vertical alignment of stacks of "thin" TLDs. The scatter in the measurements of TLDs intermediate in the stacks, reported above, resulted from individual misalignments of the square TLDs within the larger, circular holes which contained them. The fragile TLDs were inserted one at a time into the holes with vacuum tweezers, and clearance room at the corners was necessary. Square containing holes of close tolerance would correct the alignment problem but a method of manufacturing this configuration and of placing the TLDs without breakage must be devised. There are other advantages to using square holes. Without air gaps around the TLDs the shielding becomes more comparable to that of a uniform slab, especially for short range particles. A more accurate measure of depth dose for this geometry would then be possible.

In comparing the depth dose measurements with calculations (alt. 300 km, incl. 62°) of depth dose in an infinite slab-geometry, including e$^-$, p, GCR and bremsstrahlung (Watts, 1988), the experiment shows a factor of ~44 decrease in the first 0.1 g/cm^2 ^{7}LiF while the calculations show a decrease by a factor of 28.5 in the first 0.1 g/cm^2 Al. However, the true 0 g/cm^2 dose could not be measured because of the presence of the 15 μm-thick plastic windows and the fact that there was dose averaging across the TLDs. For the dose ratio between the calculated average of 0.002-0.026 g/cm^2 and 0.1 g/cm^2 Al, which is a better comparison to the experiment, the difference is a factor of 5.9. Thus the experiment gives a much steeper decline in dose over the first 0.1 g/cm^2 of shielding than does the calculation. It should be noted that the problem of misalignment of the thin TLD chips, discussed above, would give a lesser decline in the measured depth dose, so this cannot explain the difference.

The calculations show that the short range electron component is more than 99% attenuated at 0.5 g/cm^2 Al. The maximum proton plus GCR dose is less than 0.1% of the maximum electron dose but is more penetrating, so that at depths greater than 2 g/cm^2 Al the dose is dominated by protons. Between 0.5 and 3.4 g/cm^2 ^{7}LiF the measured dose decreased by ~90%, while between the same thicknesses of Al the calculated total dose decreases by ~99%. This difference may be due to the deviation of the experiment from infinite slab geometry. As stated above, close square holes for the TLD stacks would improve the modeling but there is also a component of the experimental dose which came obliquely through the sides of the 5 cm diameter Al TLD holder. Doses measured at the greater depths may have been enhanced by a factor of two or more, relative to an infinite slab geometry. Another difference with calculation derives from the difference in mass thickness between the TLD stacks and the surrounding aluminum. At 3.4 g/cm^2 in the TLDs, the aluminum walls were 4.6 g/cm^2 in depth. This reduces the measured dose by a few percent compared to a uniform slab.

The calculated dose averaged between 0.002 and 0.026 g/cm^2 was about 100 rads d^{-1}, which is somewhat below the maximum measured dose range (264 and 161 rad d^{-1} in F1 and F2). The altitude used in the calculation (300 km) is only approximate, and this will influence the comparison.

ACKNOWLEDGEMENTS

This work was supported by NASA Grant No. NCC2-521 (NASA-Ames Research Center) and NASA Grant No. NAG9-235 (NASA-Johnson Space Center, Houston). The authors would also like to thank Jim Connolly and Larry Chambers of NASA for their help.

REFERENCES

1. Benton, E.V., Peterson, D.D., Bailey, J.V. and Parnell, T.A. (1977a), High-LET particle exposure of Skylab astronauts. Health Phys. 32, pp. 15-20.

2. Benton, E.V., Henke, R.P. and Peterson, D.D. (1977b), Plastic nuclear track detector measurements of high-LET particle radiation on Apollo, Skylab, and ASTP space missions. Nucl. Track Det. 1, pp. 27-32.

3. Benton, E.V., Cassou, R.M., Frank, A.L., Henke, R.P. and Peterson, D.D. (1978a), Experiment K-206: Space radiation dosimetry on board Cosmos 936 -- U.S. portion of Experiment K-206, in : Final Reports of U.S. Experiments Flown on the Soviet Satellite Cosmos 936. (Rosenzweig, S.N. and Souza K.A., eds.), NASA TM 78526.

4. Benton, E.V., Peterson, D.D., Marenny, A.M. and Popov, V.I. (1978b), HZE particle radiation studies aboard Cosmos 782 Health Phys. 35, pp. 643-648.

5. Benton, E.V., Henke, R.P., Frank, A.L., Johnson, C.S., Cassou, R.M., Tran, M.T. and Etter, E. (1981), Experiment K-309: Space radiation dosimetry aboard Cosmos 1129: U.S. portion of Experiment K-309, in : Final Reports of U.S. Plant and Radiation Experiments Flown on the Soviet Satellite Cosmos 1129. (Heinrich, M.R. and Souza, K.A., eds.), NASA TM 81288.

6. Benton, E.V., and Henke, R.P. (1983), Radiation exposures during spaceflight and their measurement. Adv. Space Res. 3, No. 8 pp. 171-185.

7. Benton, E.V. (1984). Summary of current radiation dosimetry results on manned spacecraft. Adv. Space Res. 4, pp. 153-160.

8. Benton, E.V., Frank, A.L., Parnell, T.A., Watts, J.W., Jr. and Gregory, J.C. (1985). Radiation environment of Spacelab-1, American Inst. of Aeronautics and Astronautics conference, AIAA Shuttle Environment and Operations II, Houston, TX Nov. 13-15.

9. Benton, E.V., (1986), Summary of radiation dosimetry results on U.S. and Soviet manned spacecraft. Adv. Space Res., 6, No. 11, pp. 315-328.

10. Benton, E.V., and Parnell, T.A. (1987), Space radiation dosimetry on U.S. and Soviet manned missions, NATO Advanced Study Institute, "Terrestrial Space Radiation and its Biological Effects," Corfu, Greece: 11-25 Oct.

11. Kovalev, E.E., Benton, E.V. and Marenny, A.M. (1981), Measurement of LET spectra aboard Cosmos 936 biological satellite. Rad Prot. J., 1, pp. 169-173.

12. Peterson, D.D., Benton, E.V. and Tran, M. (1978), K-103: HZE particle dosimetry, in : Final Reports of U.S. Experiments Flown on the Soviet Satellite Cosmos 782. (eds., Rosenzweig, S.N. and Souza, K.A.), NASA TM 78525.

13. Watts, J.W., Jr. (1988) Marshall Spaceflight Center, Huntsville, AL, private communication.

Table 1

TLD DOSE RATES AS A FUNCTION OF DEPTH

Detector	TLD Stacks	Depth in ^7LiF (g/cm^2) +$2.16 \times 10^{-3} g/cm^2$ Plastic*	Tissue Absorbed Dose-Rate (rad/day)
K-6-25 F1	1+2	0.012	264
K-6-25 F2	1+2	0.012	161
K-6-25 F1	1+2	0.1	5.3
K-6-25 F2	1+2	0.1	4.4
K-6-25 F1	1+2	0.5	0.40
K-6-25 F2	1+2	0.5	0.29
K-6-25 F1	1+2	1.0	0.13
K-6-25 F2	1+2	1.0	0.076
K-6-25 F1	3	1.0	0.17
K-6-25 F2	3	1.0	0.13
K-6-25 F1	1+2	2.0	0.049
K-6-25 F2	1+2	2.0	0.038
K-6-25 F1	3	2.0	0.060
K-6-25 F2	3	2.0	0.046
K-6-25 F1	1+2	3.4	0.038
K-6-25 F2	1+2	3.4	0.028
K-6-25 F1	3	3.4	0.040
K-6-25 F2	3	3.4	0.032
K-6-24		Inside Spacecraft	0.0248 +/-0.0010

*Kapton

Table 2

PNTD RESULTS FROM COSMOS 1887

Experiment	Stack	Min. Shielding in plastic (g/cm^2)	Spectrum type	Flux ($cm^{-2}s^{-1}sr^{-1}$) x 10^{-4}	Dose (mrad d^{-1})	Dose equiv. rate (mrem d^{-1})
K-6-25	1-a	0.195	TOT	34.3	5.25	30.8
			GCR	2.50	1.20	16.0
			SR	31.8	4.05	14.8
	-b	0.436	TOT	20.0	3.65	22.5
			GCR	1.53	0.74	8.5
			SR	18.5	2.91	14.0
	-c	0.762	TOT	13.2	2.79	20.1
			GCR	2.24	1.10	12.6
			SR	10.9	1.69	7.5
	-d	1.33	TOT	10.3	2.50	19.8
			GCR	2.79	1.18	13.7
			SR	7.47	1.32	6.1
	2-a	0.319	TOT	21.3	3.52	19.9
			GCR	1.81	0.83	9.5
			SR	19.5	2.69	10.4
K-6-24	--- Inside Spacecraft		TOT	4.25	1.27	11.4
			GCR	1.38	0.63	7.1
			SR	2.87	0.64	4.3

*LET_{∞}•$H_2O \geq 4$ keV μm^{-1}

Table 3

RADIATION MEASUREMENTS ON JOINT US/USSR COSMOS FLIGHTS

FLIGHT NO.	782	936	1129	1887
Launch Date	Nov. 1975	Aug. 1977	Sept. 1979	Sept. 1987
Duration (d)	19.50	18.30	18.56	12.63
Inclination (^{o})	62.8	62.8	62.8	62.8
Altitude (km Apogee/Perigee	405/226	419/224	394/226	406/224
HEAVY PARTICLES Flux Inside ($cm^{-2}s^{-1}sr^{-1}$)	$8.7\pm1.4\times10^{-6}$*	$5.1\pm1.0\times10^{-6}\Delta$	$6.1\pm0.1\times10^{-7}\nabla$	$4.25\pm0.24\times10^{-4}$ †
Flux Outside ($cm^{-2}s^{-1}sr^{-1}$)			$1.21\pm0.02\times10^{-6}\nabla$	$3.43\pm0.22\times10^{-3}$ †
Dose Equivalent Rate Inside (mrem d^{-1})				11.4±0.7
Outside (mrem d^{-1})				30.8±2.0
TLD DOSE RATE Inside (mrad d^{-1})		25.6±1.3	18.0±3.6 ††	24.8±1.0
Outside (max.) (mrad d^{-1})				$2.64\pm0.28\times10^{5}$
NEUTRONS Thermal Flux (cm^{-2} d^{-1})		$1.9\pm0.4\times10^{4}$	$2.7\pm0.5\times10^{4}$	
Resonance Flux (cm^{-2} d^{-1})		$6.5\pm3.2\times10^{4}$	$7.5\pm3.8\times10^{4}$	
High Energy Flux (cm^{-2} d^{-1})		$1.1\pm$ -$\times10^{5}$	$1.1\pm$-$\times10^{5}$	
Thermal Dose (mrem d^{-1})		0.020±0.004	0.028±0.006	
Resonance Dose (mrem d^{-1})		0.32±0.16	0.40±0.20	
High Energy Dose (mrem d^{-1})		6.8± ?	6.8± ?	

*LET_{∞}•H2O ≥ 105 keVμm^{-1}; .100 µm range. ΔLET_{∞}•H_2O ≥ 106 keV μm^{-1}; .180 µm range.

∇Different processing; results not comparable to other flights.

†LET_{∞}• H_2O ≥ 4 keV μm^{-1}; >100 µm range. ††Detectors irradiated during return transportation.

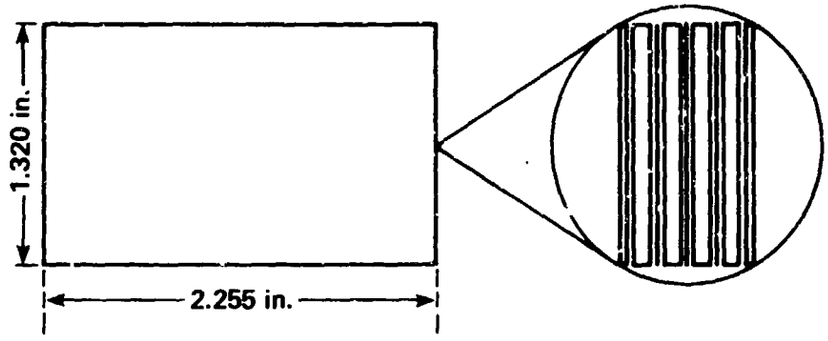

(a) SIZE OF X AND Y DETECTORS
(16 X CR-39; 8 X LEXAN)

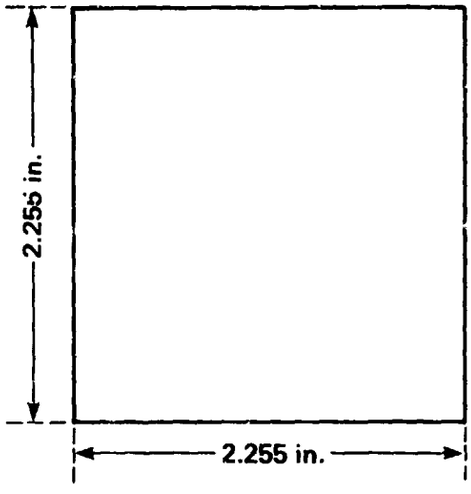

(b) SIZE OF Z DETECTOR (39 X CR-39; 4 X TUFFAK)
THE TOTAL THICKNESS OF THIS STACK IS 1.000 in.
THE COMPONENTS OF THE STACK ARE:
LEXAN (250 μm)
CR-39 (625 μm)
SEPARATED BY PC FOILS (8 μm)
·
· (39 PAIRS)
·
TUFFAK (4 X 254 μm)
LEXAN (250 μm)

Figure 1: A sketch of the PNTD stacks in Experiment K-6-24.

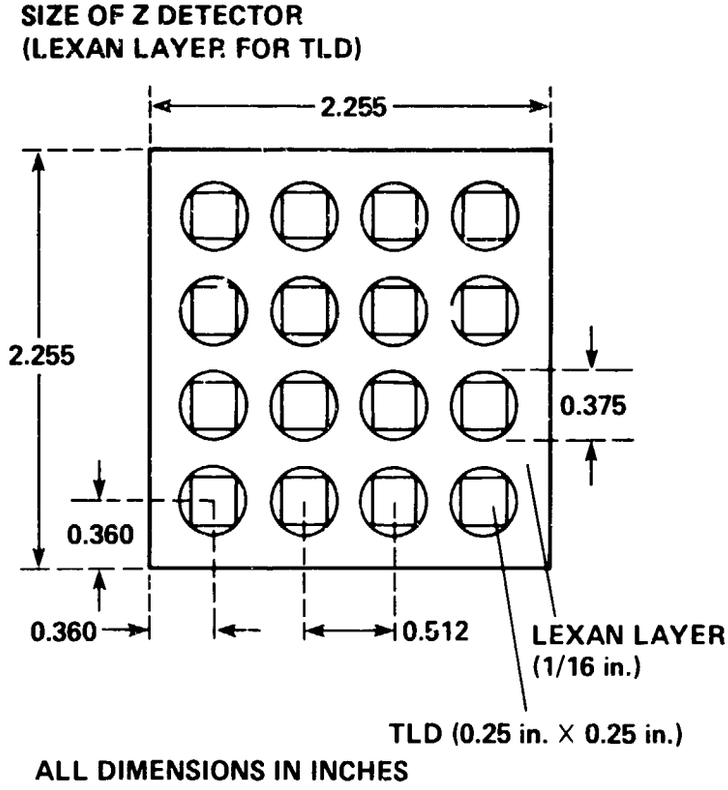

Figure 2: A sketch of the TLD array in Experiment K-6-24.

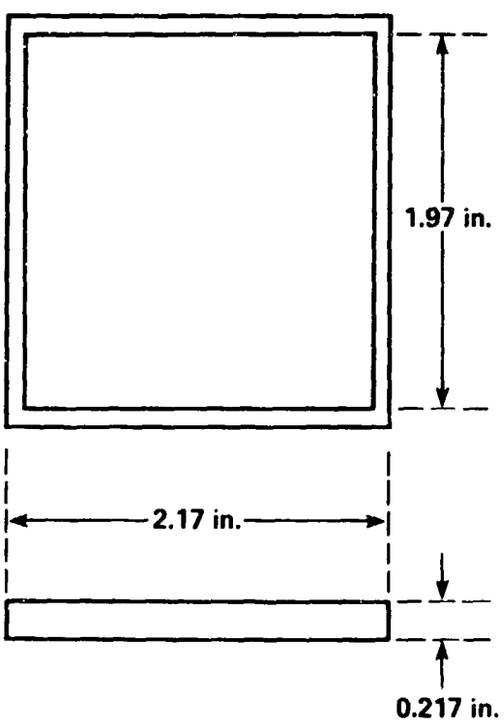

Figure 3: A sketch of the nuclear emulsion package in Experiment K-6-24.

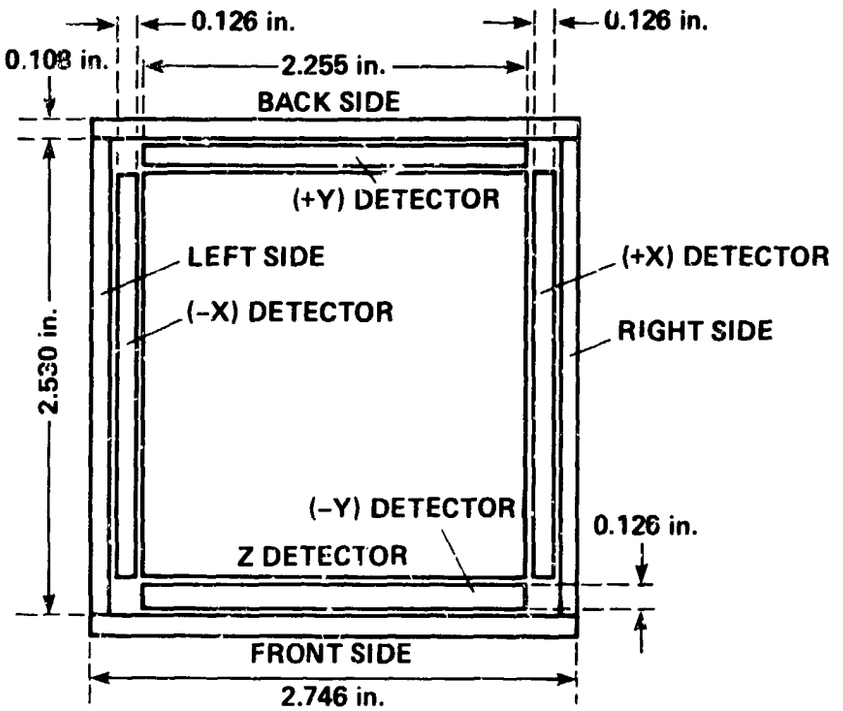

(a) TOP VIEW (SIDES ARE LEXAN 0.108 in. THICK)

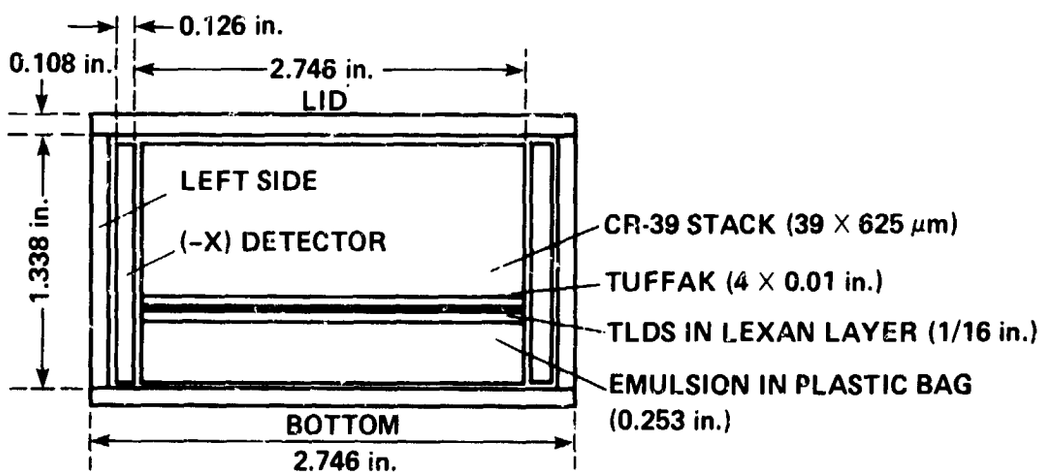

(b) SIDE VIEW

KOSMOS 87

(a) TOP VIEW OF THE OPEN LEXAN BOX

(b) SIDE VIEW INCL. Z DETECTOR STACK ALL DIMENSIONS IN INCHES

Figure 4: A sketch of the detector array in Experiment K-6-24.

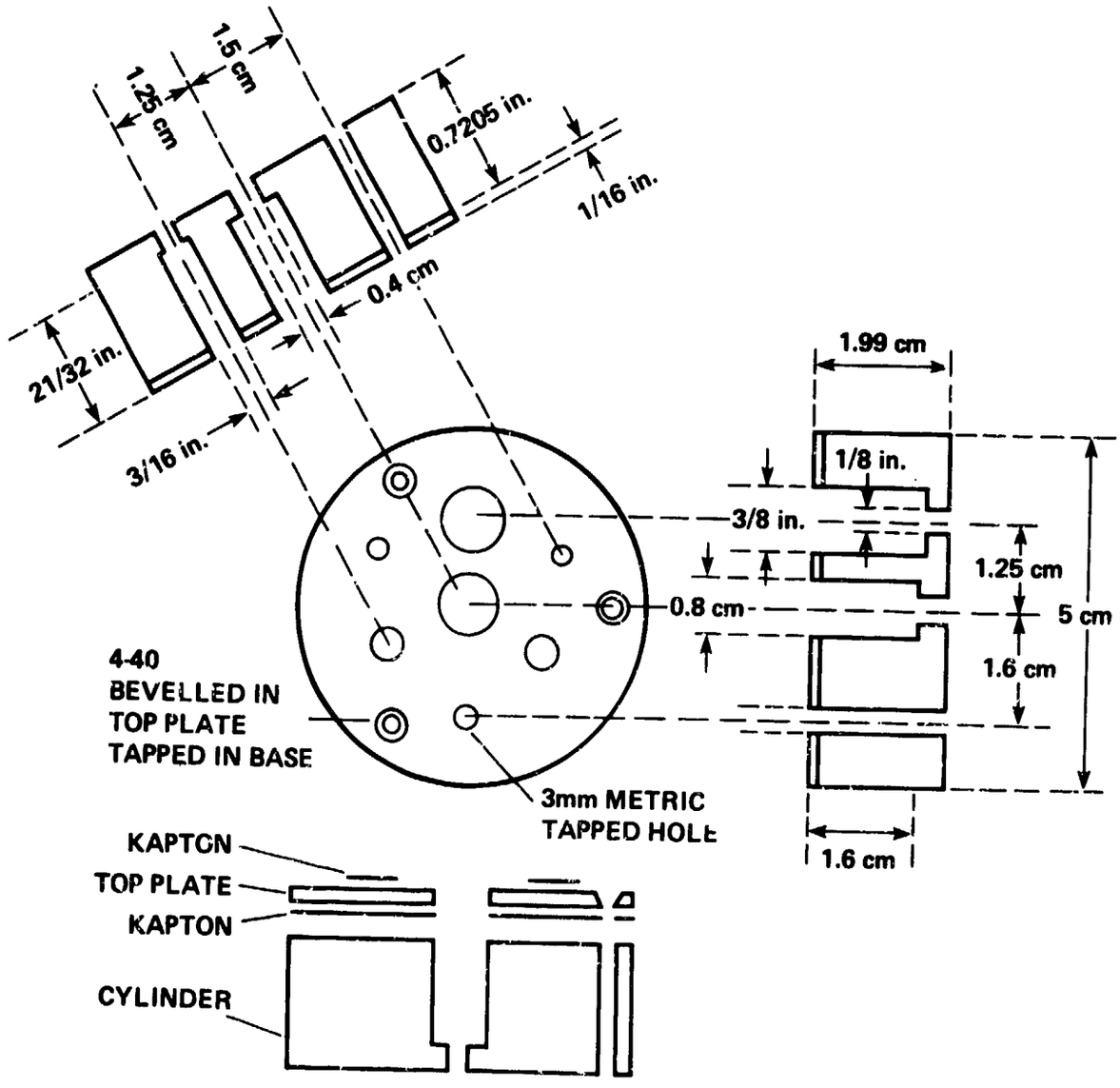

Figure 5: A sketch of the aluminum TLD stack container in Experiment K-6-25.

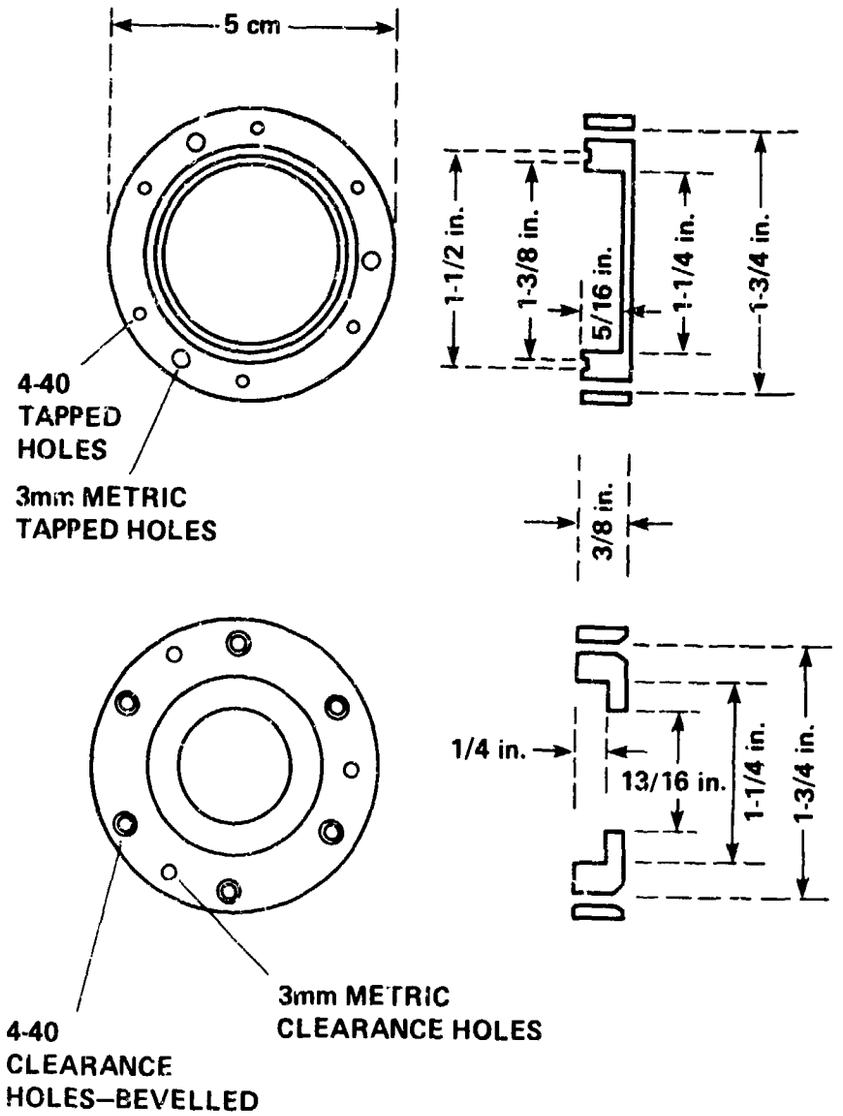

Figure 6: A sketch of the aluminum, sealed container for PNTD stacks in Experiment K-6-26 A.

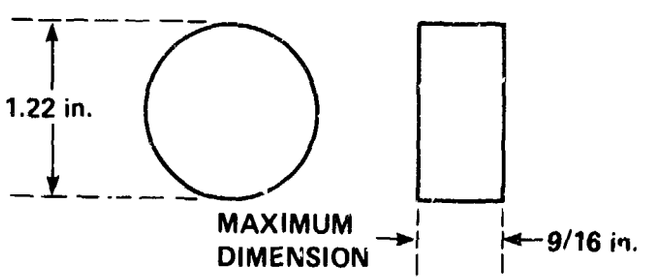

Figure 7: Dimensions of plastic nuclear track detector stacks in Experiment K-6-26 A.

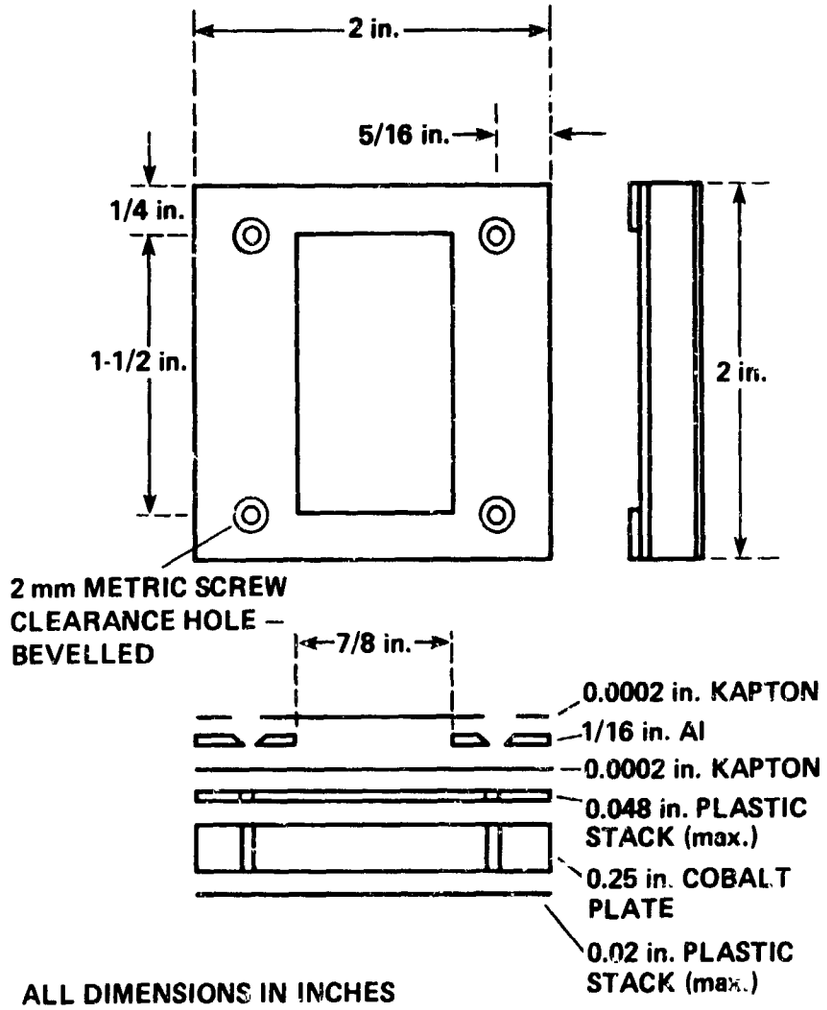

Figure 8: A sketch of the detector array in Experiment K-6-26 B.

ORIGINAL PAGE
BLACK AND WHITE PHOTOGRAPH

Figure 9: "Clam Shell" detector container flown on Cosmos 1887 showing effects of high temperature on several detector stacks.

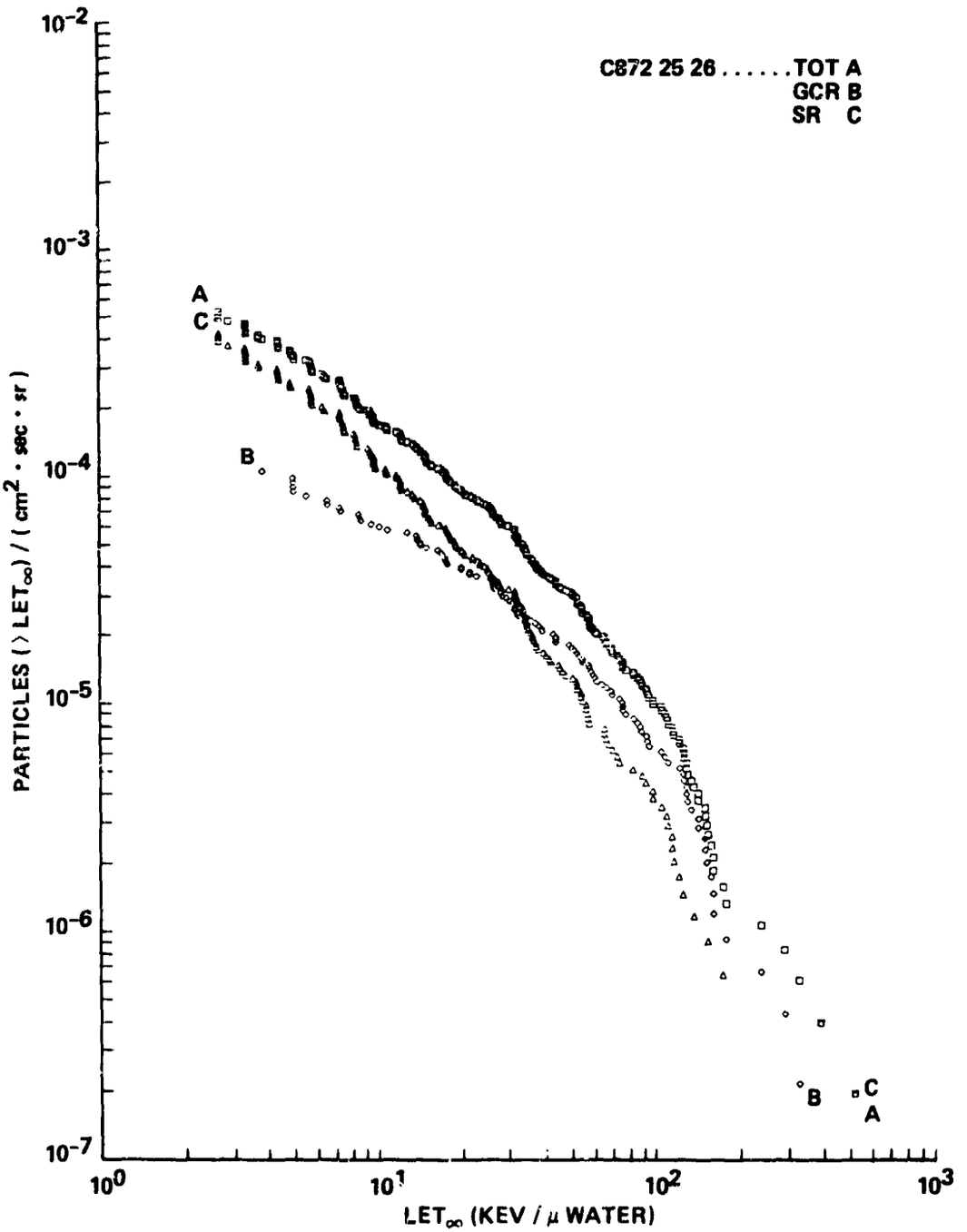

Figure 10: Integral LET flux spectra for Experiment K-6-24 (inside spacecraft). Average of three orthogonal detectors.

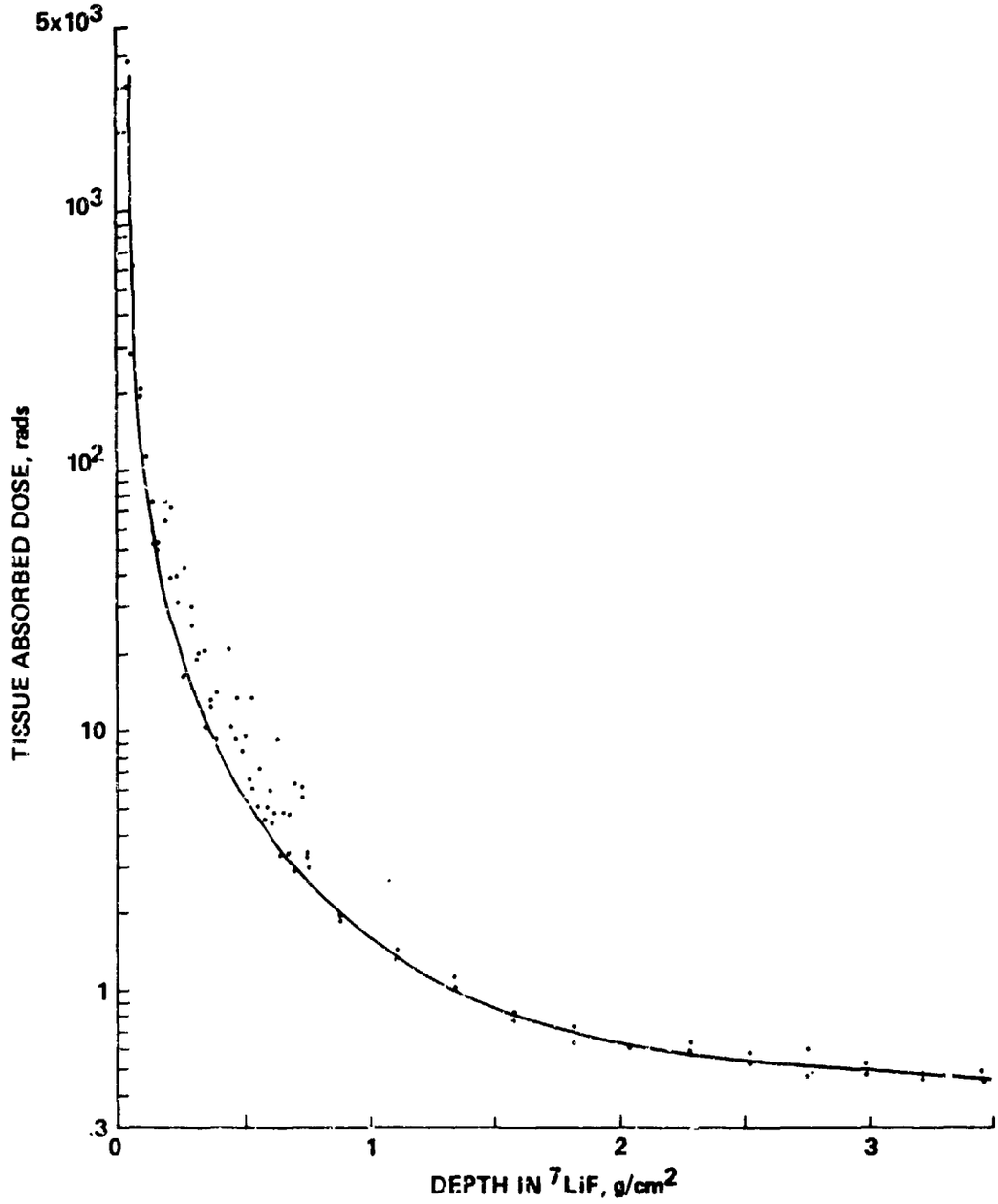

Figure 11: A plot of the depth-dose measurements for TLD stacks 1 and 2 from Experiment K-6-25 F1. Above the ^{7}LiF stacks were double windows of Kapton plastic totaling 15 μm (2.16×10^{-3} g/cm^2).

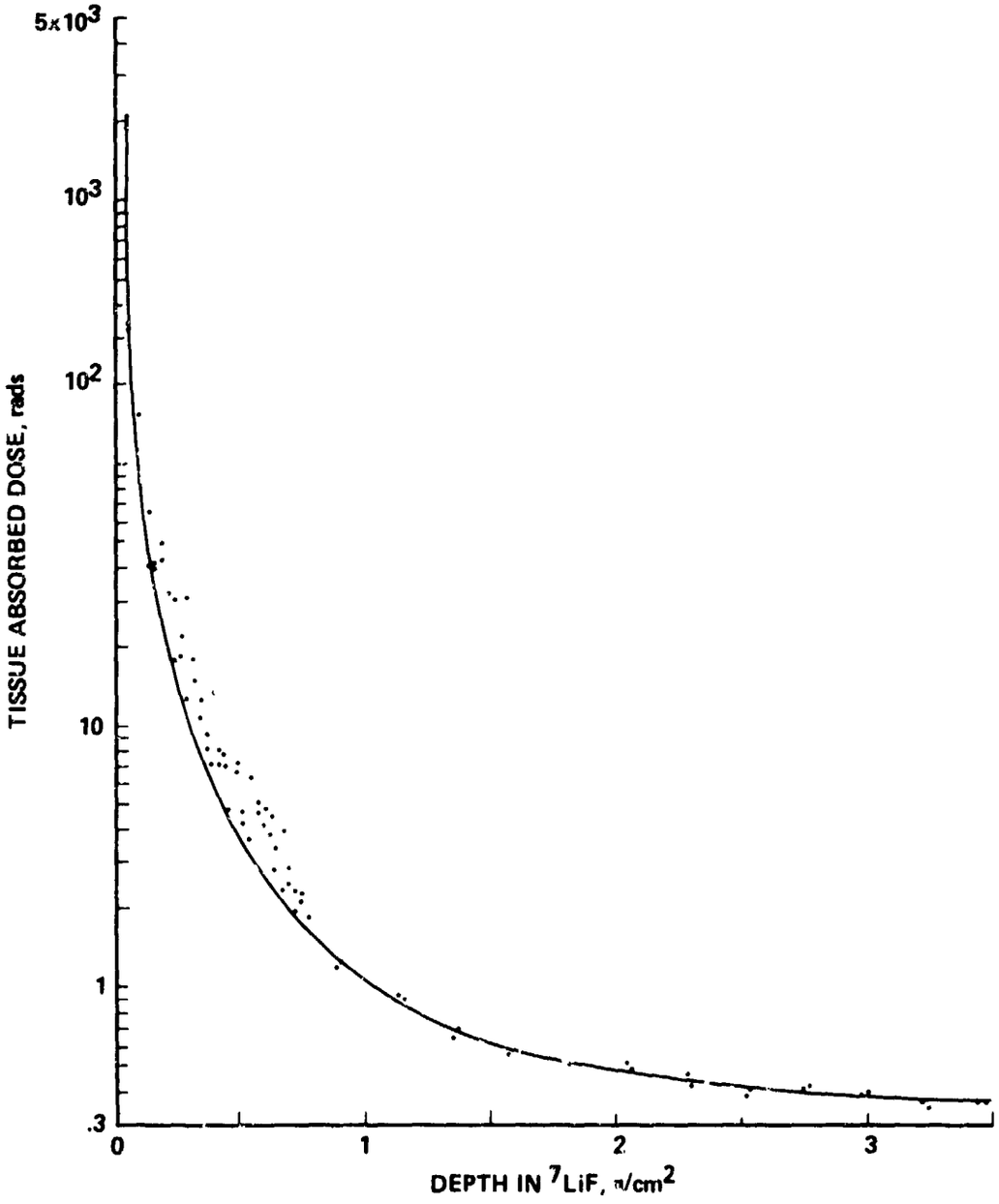

Figure 12: A plot of the depth-dose measurements for TLD stacks 1 and 2 from Experiment K-6-25 F2. Above the ^{7}LiF stacks were double windows of Kapton plastic totaling 15 μm (2.16×10^{-3} g/cm^2).

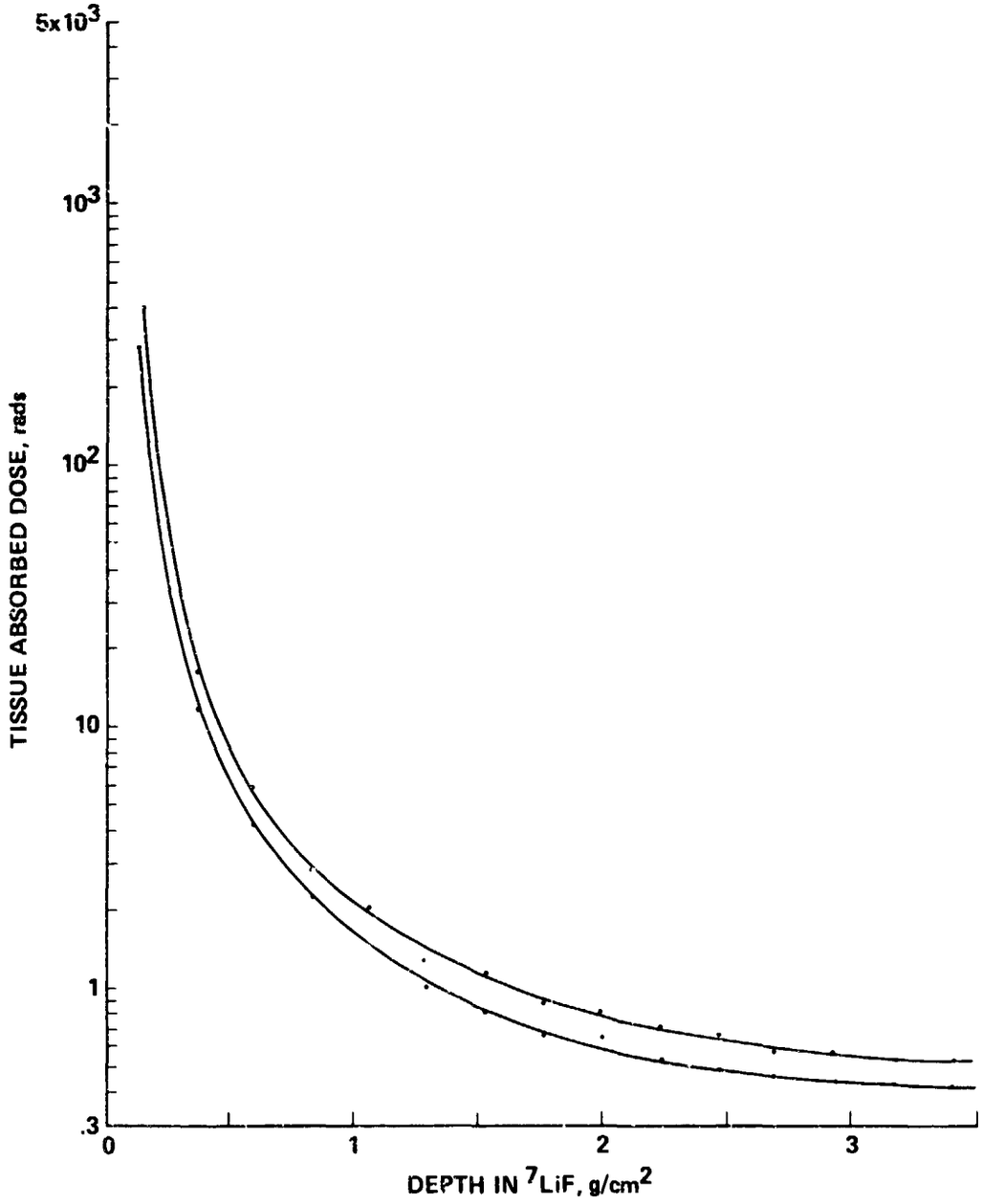

Figure 13: Plots of the depth-dose measurements for TLD stacks 3 from Experiments K-6-25 F1 and F2. Above the ^{7}LiF stacks were double windows of Kapton plastic totaling 15 μm (2.16×10^{-3} g/cm^2).

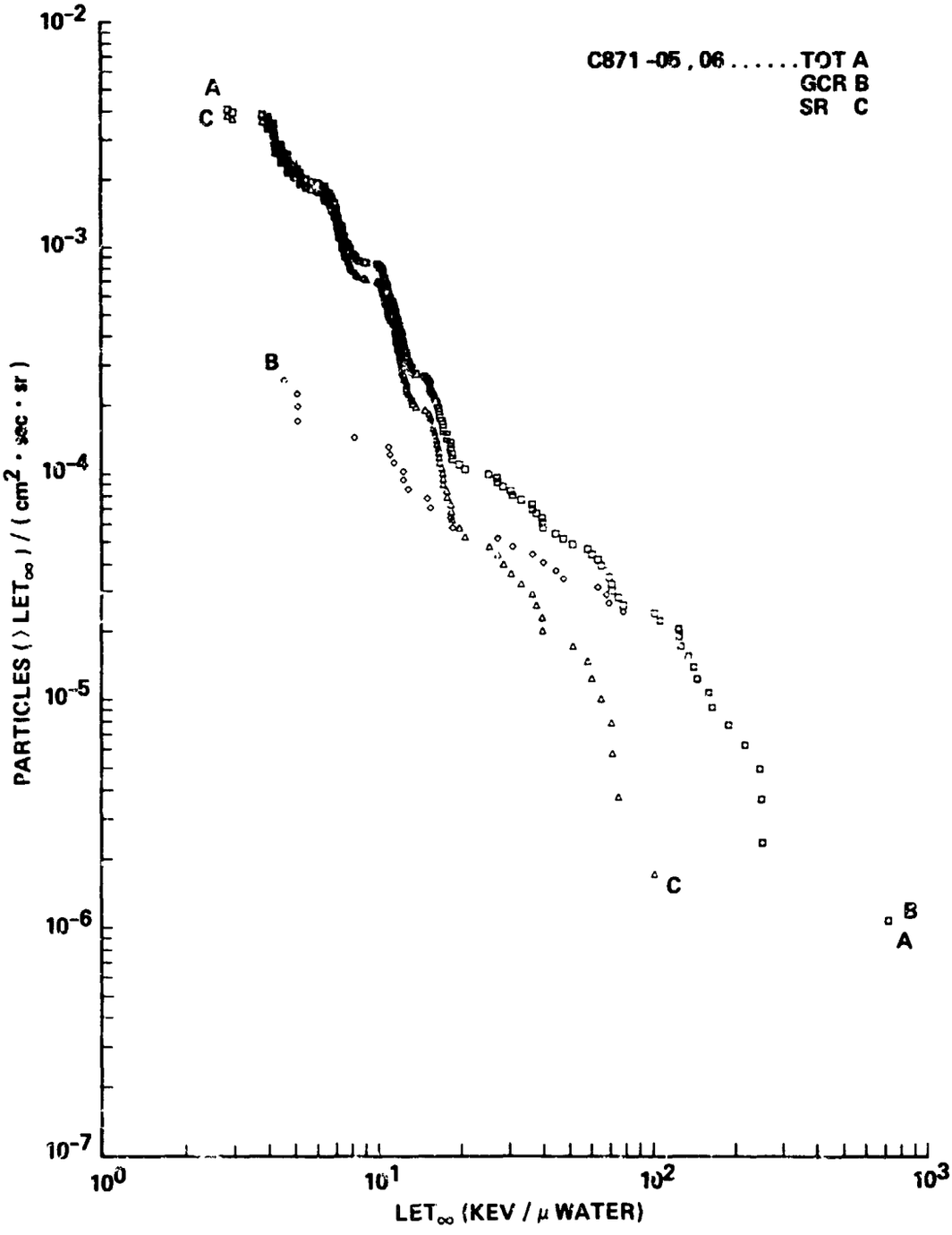

Figure 14: Integral LET flux spectra for Experiment K-6-26 A, PNTD stack F1 (outside the spacecraft). Shielding was 0.195 g/cm^2 of plastic.

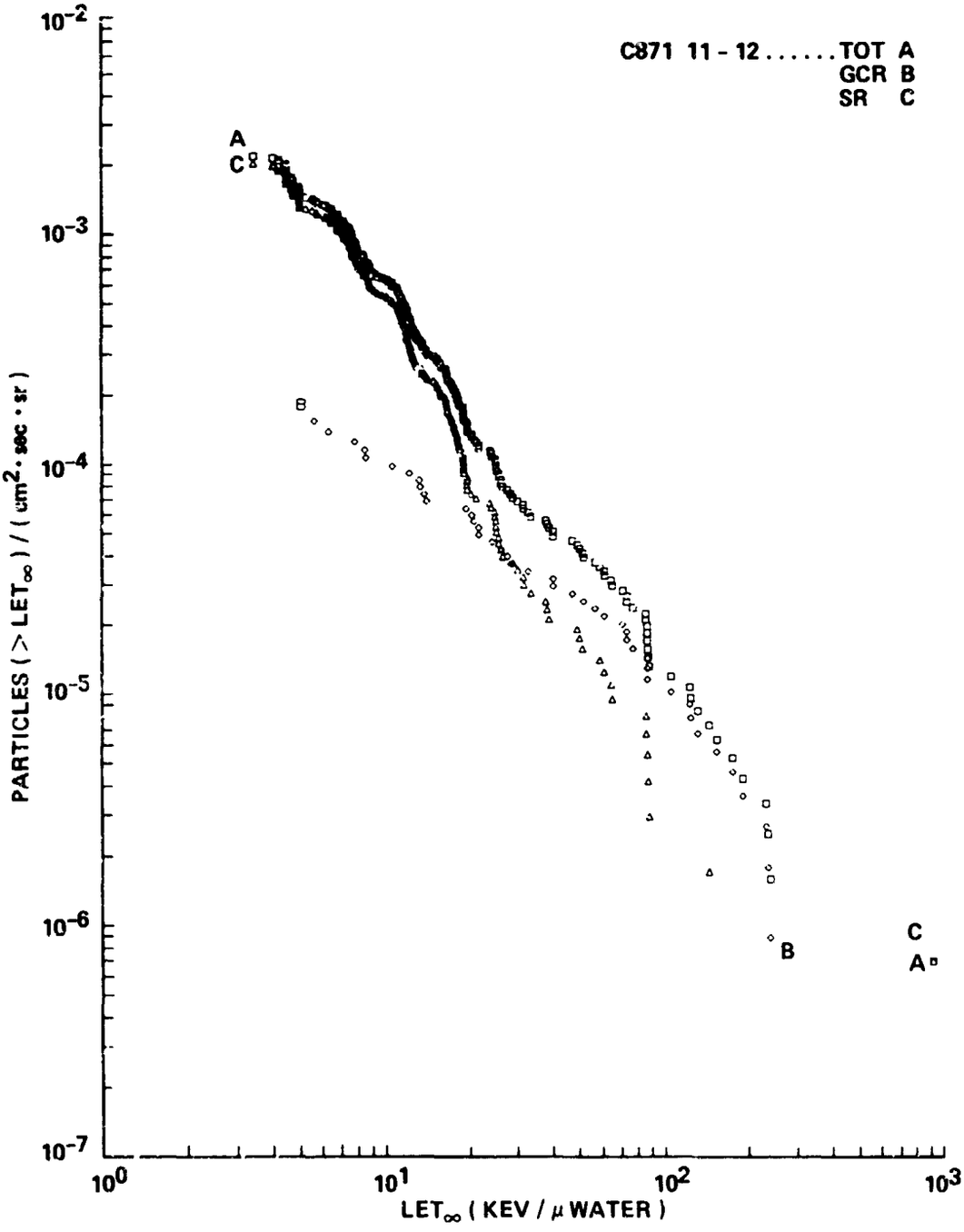

Figure 15: Integral LET flux spectra for Experiment K-6-26 A, PNTD stack F1 (outside the spacecraft). Shielding was 0.436 g/cm^2 of plastic.

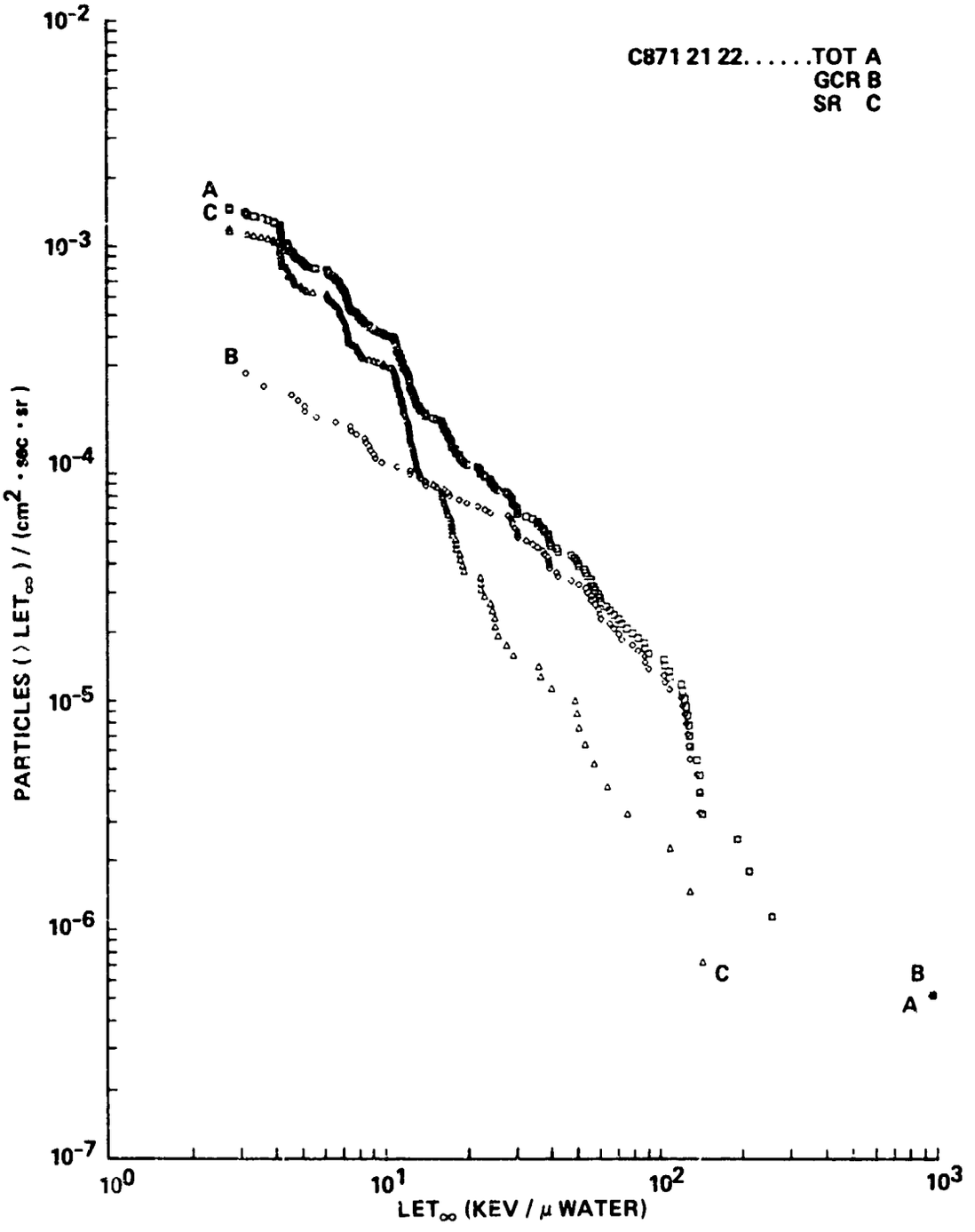

Figure 16: Integral LET flux spectra for Experiment K-6-26 A, PNTD stack F1 (outside the spacecraft). Shielding was 0.762 g/cm^2 of plastic.

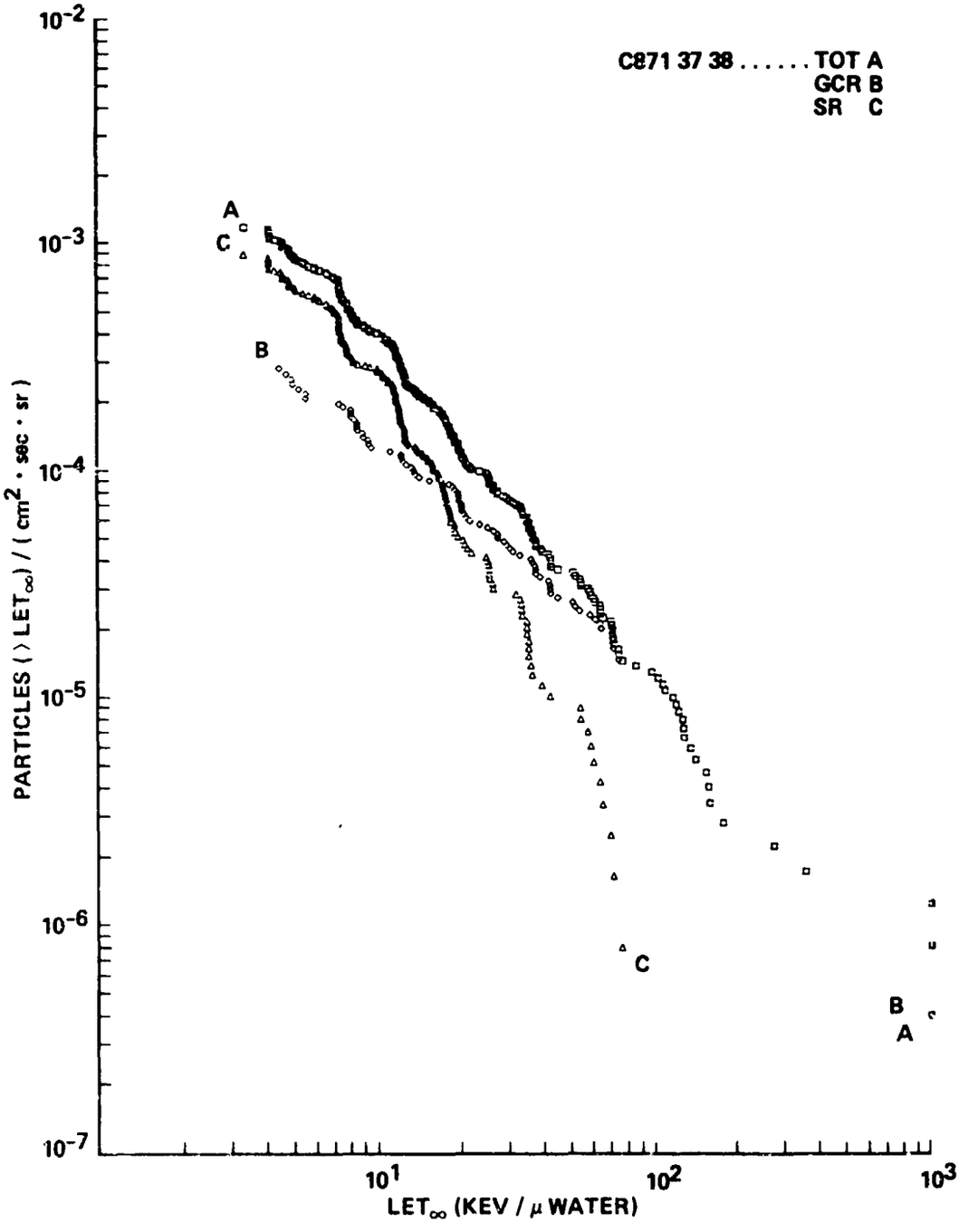

Figure 17: Integral LET flux spectra for Experiment K-6-26 A, PNTD stack F1 (outside the spacecraft). Shielding was 1.33 g/cm^2 of plastic.

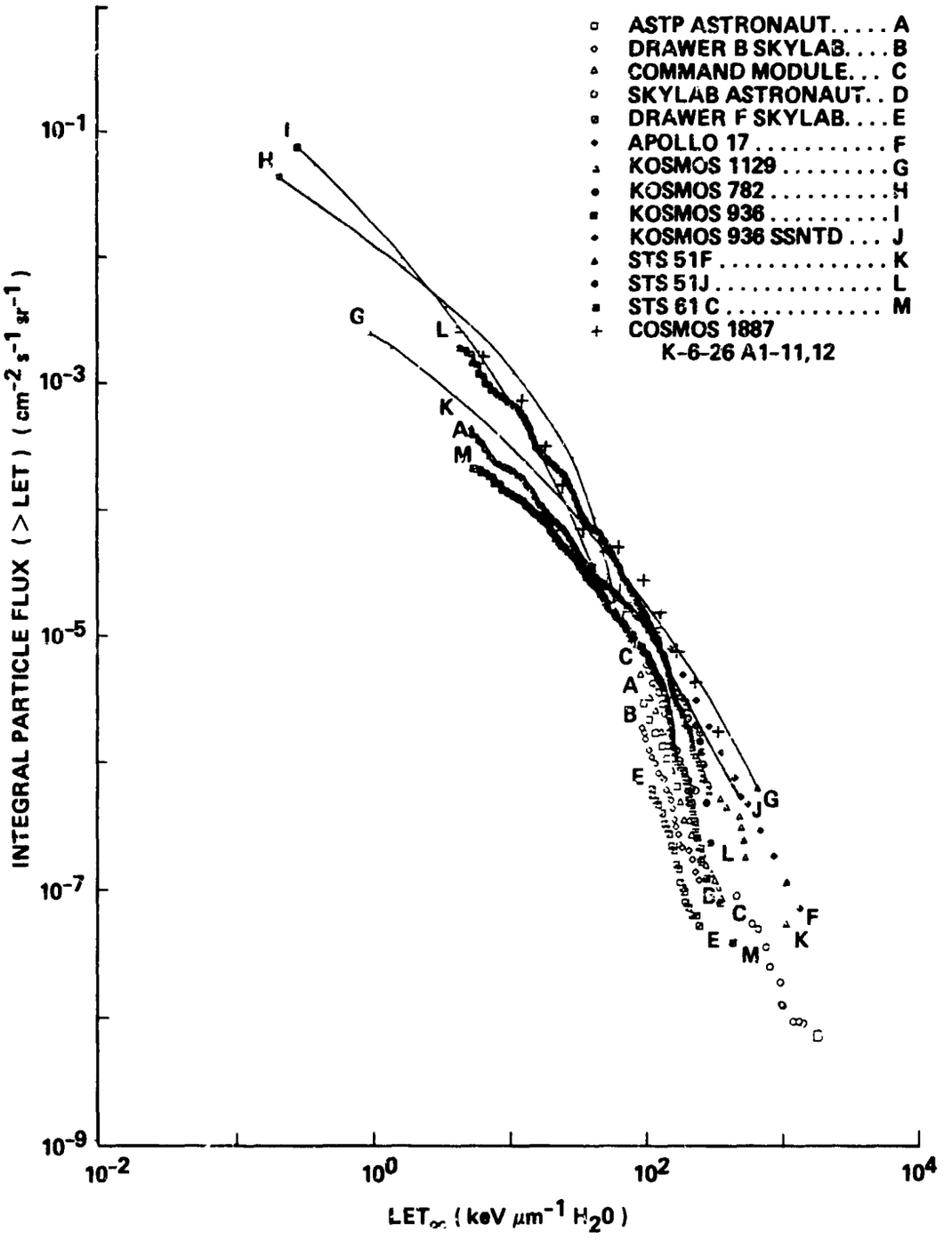

Figure 18: Integral LET spectra showing number of particles as a function of LET_∞ in water for various U.S. and Soviet flights. Not data for Cosmos 1887 (crosses). /Fenton and Parnell, 1988./